A&A 464, 1015–1022 (2007)
DOI: 10.1051/0004-6361:20065638
© ESO 2007

Astronomy & Astrophysics

# Inferences from the kinematic properties of 6.7 GHz methanol masers

D. J. van der Walt[1], A. M. Sobolev[2], and H. Butner[3]

[1] Unit for Space Research, North-West University, Private Bag X6001, Potchefstroom, South Africa
e-mail: fskdjvdw@puk.ac.za
[2] Ural State University, Lenin Ave. 51, Ekaterinburg, Russia
e-mail: Andrey.Sobolev@usu.ru
[3] Joint Astronomy Centre, 660 N. A'ohoku Place, University Park, Hilo, Hawaii, USA
e-mail: h.butner@jach.hawaii.edu

Received 19 May 2006 / Accepted 11 January 2007

**ABSTRACT**

*Context.* It is now well established that the strong and widespread 6.7 GHz methanol masers are associated with young high mass stars. A still unsolved question is where in the circumstellar environment the masers arise.
*Aims.* We address this question by considering an ensemble of rest frame maser velocities of 337 maser features.
*Methods.* The CS(2−1) spectra of 63 methanol maser sources were used to derive systemic velocities and velocity dispersion of the thermal gas. Using the systemic velocities and the velocities of the 337 maser features in the 63 sources, a single distribution of rest frame maser velocities was constructed. This distribution as well as other kinematic information about the masers are used to evaluate four proposed scenarios for where the masers might arise in the circumstellar environment.
*Results.* It is shown that kinematically the masers are not associated with hot cores. We also argue that the scenario in which the masers are associated with an external generated planar shock that propagates into a rotating core cannot explain the observed kinematic properties of the masers. It was found that a simple Keplerian-like disk model is consistent with the observed distribution of rest frame maser velocities. Although outflows have the potential to explain the data, it was not possible to fully test this possibility due to the diverse nature of outflows.
*Conclusions.*

**Key words.** masers – stars: formation – ISM: molecules

## 1. Introduction

Over the last decade or so, class II methanol masers, and in particular the strong 6.7 GHz masers, proved to be very useful indicators of high mass star formation in the Galaxy (Ellingsen 2006). At present more than 500 6.7 GHz methanol masers sources are known (Malyshev & Sobolev 2003; Xu et al. 2003; Pestalozzi et al. 2005).

One of the still outstanding questions about the 6.7 GHz methanol masers is where in the circumstellar environment they originate. Before it is possible to fully exploit the masers as probes of the star forming region, is it necessary to first find an answer to this question. Since their discovery, a number of possibilities for where the masers might arise have been proposed by various authors.

Historically, the first statement on the nature of class II masers was that they arise from the dense warm molecular material surrounding the compact HII regions excited by newly formed massive stars (Menten 1991). High resolution imaging of methanol masers (Norris et al. 1993, 1998) showed that for some maser sources the maser spots form linear structures and exhibit velocity gradients. Norris et al. (1993, 1998) argued that the linear structures were consistent with rotating disks of masers seen edge-on. Within the framework of the disk hypothesis Durisen et al. (2001) suggested that the masers are associated with gravitational instabilities in the disk. Slysh et al. (1999a) postulated the masers to be associated with icy planets in circumstellar accretion disks. It should also be noted that the correlation of turbulent velocities in disks but also in general, can explain some of the observed properties of masers (Sobolev et al. 1998; Wallin et al. 1998). A survey by Walsh et al. (1998) found that 36 out of 97 maser sites were linearly extended and in some cases show linear velocity gradients along the lines of maser features. These authors, however, suggested that the masers arose behind shock fronts. Dodson et al. (2004) elaborated on the shock model and proposed that their observations can be explained in terms of an external generated planar shock propagating through a rotating core. Recently, Minier et al. (2000) presented VLBI observations of 6.7 and 12.2 GHz methanol masers in 14 northern star-forming regions. In 10 cases the methanol masers show elongated morphologies and also exhibit linear velocity gradients. Minier et al. (2000) came to the conclusion that although their results can be interpreted in terms of the masers residing in rotating disk-like structures, other models such as accelerating outflows should also be considered. De Buizer (2003) tested the circumstellar disk hypothesis by searching for $H_2$ outflow signatures from massive young stellar objects with linearly distributed methanol maser spots and conclude that the masers are most likely associated with outflows rather than with circumstellar disks. Recently van der Walt (2005) argued on the basis of the similarity between the estimated lifetimes of methanol masers and hot cores, as well as the abundance of methanol in hot cores, that the masers might be associated directly with hot cores. Minier et al. (2001) and De Buizer et al. (2005) also pointed to such a possible association. The discovery of a ring of masers in G23.657-0.127 by Bartkiewicz et al. (2005) adds

Article published by EDP Sciences and available at http://www.aanda.org or http://dx.doi.org/10.1051/0004-6361:20065638

a new spatial distribution of maser spots not seen before. These authors interpret this spatial arrangement of maser spots as being due the masers lying on the edge of an expanding spherical bubble or in a rotating disk seen nearly face-on. Sutton et al. (2001) also interpreted the class II masers in W3(OH) as possibly being associated with an expanding spherical shell surrounding the HII region.

Thus, in spite of significant effort that went into trying to understand where in the circumstellar environment the masers originate, no clear answer has yet emerged. Needless to say that, whichever scenario(s) is correct, in addition to explaining the kinematic properties of the masers, the conditions required to pump the masers (Sobolev & Deguchi 1994; Cragg et al. 2002, 2005) should also be met.

In this paper we add to the present discussion about the question of where in the circumstellar environment the masers arise. Rather than focusing on the high resolution properties of the masers spots in individual maser sources as was done by many authors up to now, we here consider the *joint* (collective) line-of-sight kinematic properties of a large number (337) of maser features as evidenced by the distribution of the line-of-sight velocities of the masers in the rest frames of the molecular cores with which they are associated. The basic motivation for this approach is that if the methanol masers trace the same well-defined kinematic structures, say e.g. disks, in different star forming cores, it can be expected that the distribution of rest frame line-of-sight velocities of a large number of masers features will reflect the kinematics of the structures where they originate. By following this approach we hope to avoid the problem formulated by Beuther et al. (2002) that "*We cannot determine accurately in any source of this sample whether the maser emission is produced in disks, outflows, or shock waves. This stresses that kinematic interpretations of different maser features are difficult and not as straightforward as sometimes supposed in the past. We believe that the approach of kinematic interpretation of different maser features works only in a limited number of sources with a favorable geometry with respect to the observer, and then especially when proper motion observations are available*".

Our analysis shows that, purely from a kinematic point of view, the masers are most likely not associated with hot (>100 K) gas as found in hot molecular cores. We also show that the external generated planar shock model of Dodson et al. (2004) cannot explain the observed kinematic properties of methanol masers. The predictions of a Keplerian-like disk were found to be consistent with the observed kinematic properties of the masers. Although outflows are a common property of the sources in our sample, the complex geometry of outflows makes it difficult at this time to make definite conclusions about this possibility.

## 2. Data and the distribution of line-of-sight maser velocities

To construct the distribution of rest frame maser velocities it is necessary to transform the velocities of individual maser features to the rest frames of the clouds/cores with which they are associated. This requires the determination of the systemic velocities of the maser sources that will be used. A good tracer of dense gas, and therefore of the cores with which the masers are associated, is CS. Although single dish CS(2−1) data, which include systemic velocities and line widths, have been published for many maser sources (e.g. Bronfman et al. 1996), a reliable determination of the systemic velocities requires knowledge of what

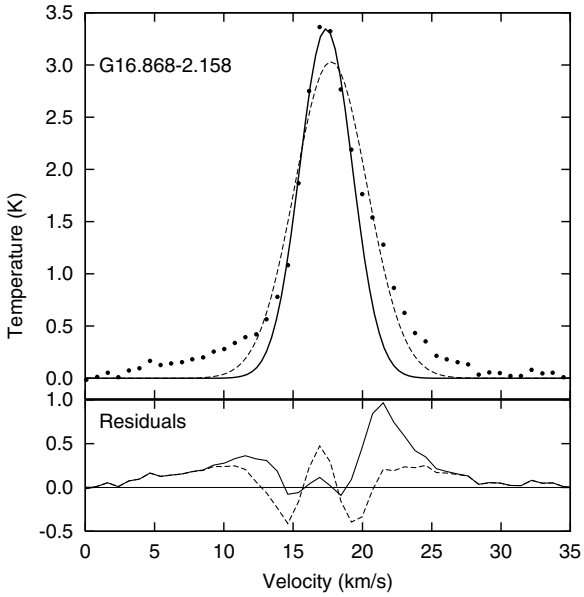


**Fig. 1.** Example of two possible Gaussian fits to a CS(2−1) line profile with high velocity wings on the red and blue side. The dashed line is the fit when the wings are included when making the fit. The solid line is the fit when the wings are excluded. Excluding the wings allows an acceptable fit to the center of the line.

the individual line profiles looks like. In the case where the line profile is Gaussian, the systemic velocity can be found by fitting a Gaussian to the line. On the otherhand, fitting a Gaussian to a line that shows, for example, evidence of strong self-absorption or high velocity wings, can lead to a wrong estimate of the systemic velocity. For this reason we used the CS(2−1) spectra of 119 methanol maser sources obtained with the Kitt Peak 12 m telescope[1] by HB during the period April 2001 to February 2002 and by DJvdW during May 14−16, 2005. The spectra of the 119 sources were inspected individually and 63 sources were selected on the basis that their CS(2−1) spectra could be fitted by a single Gaussian or where, after removal of high velocity wings, the central part of the line could be fitted by a Gaussian. The velocities of individual 6.7 GHz methanol maser features for the 63 sources were taken from Walsh et al. (1998), Szymczak et al. (2000), and Caswell et al. (1995).

We illustrate the fitting of a Gaussian to the central part of a line that shows high velocity wings on both the red- and blue sides with the example of G16.868-2.158 (see Fig. 1). The dashed line in the upper panel shows the best fit to the data with the high velocity wings included. That this fit is not acceptable can be seen by inspecting the residuals (bottom panel, dashed line). It is seen that the residuals show a strong oscillatory behavior due to the fact that there are groups of data points that lie systematically above or below the fitted line. For the fit to be acceptable, the residuals should scatter randomly around zero. A more formal statistical analysis of the correctness of the fit can be done in terms of the Runs Test but we will not follow that procedure here. Inspection furthermore shows that the peak of the Gaussian fit does not coincide with the maximum as suggested by the data points which results in a wrong estimate of the systemic velocity. The Gaussian fit also completely underestimates the peak temperature of the line. A better, but still not perfect, fit to the central part of the line where the wings have no effect,

[1] The Kitt Peak 12 Meter telescope is operated by the Arizona Radio Observatory (ARO), Steward Observatory, University of Arizona.

was found by systematically removing data points starting from the high velocity sides of the wings and to follow the improvement of the fit as measured by the reduced chi-squared value. The solid line in the top panel gives the final fit to the central part of the line and in the bottom panel the residuals for this fit are shown. It can be seen that, compared to the dashed line, the peak of the line is now much better fitted and the residuals are significantly smaller over that part as well. Comparison of the two fits also show that the fit to the data where the wings are included gives rise to a greater line width than when the wings are not included in the fit. This procedure to fit Gaussians to the CS(2−1) lines was followed for all sources where the line showed high velocity wings and where the central part could be fitted with a Gaussian.

Using the above procedure we estimated the systemic velocities of the 63 sources and constructed the distribution of rest frame velocities for the 337 maser features in the 63 sources. In Table 1 we present the derived systemic velocities, the width of the CS(2−1) line as measured by the standard deviation of the fitted Gaussian, and the velocities of the individual maser features obtained from the literature. The resulting distribution of rest frame maser velocities is shown in Fig. 2. Comparison of the means and standard deviations of the blue- and red shifted sides of the distribution suggests that there is no difference between the two sides and that it is valid to construct an average distribution (dashed histogram in Fig. 2). Irrespective of its interpretation, the distribution seems to be well behaved in the sense that it shows a single well defined maximum around 0 km s$^{-1}$ and a well behaved decrease in the number of masers towards higher velocities. Using the red- and blueshifted data together we find an average cloud rest frame velocity of 0.45 km s$^{-1}$ and a standard deviation of 4.8 km s$^{-1}$. We note that Slysh et al. (1999b) basically followed the same procedure as we did here when constructing a distribution of rest frame maser velocities for the strongest maser features in 157 maser sources.

## 3. Evaluation of the different scenarios

In this section we now discuss, in view of the distribution of the rest frame velocities as shown in Fig. 2, the merit of the different scenarios of where in the circumstellar environment the methanol masers arise. Our basic assumption in the analysis that follows is that the masers are associated with only one of the four possibilities, i.e. hot cores, disks, external generated planar shocks propagating into the core, or outflows. This assumption is certainly not beyond criticism and it has to be kept in mind that there might be examples where the 6.7 GHz methanol masers arise in more than one of the possible environments.

### 3.1. Hot cores

In Fig. 3 we show the example of G29.96-0.02 where we compare the CS(2−1) thermal line profile with the associated 6.7 GHz methanol maser spectrum. It is seen that the velocities at which the masers occur overlap to a large extent with the $3\sigma$ velocity range of the thermal gas. Although CS is not a typical hot core molecule, a comparison of the velocities of the maser features with the associated thermal line profiles of typical hot core molecules such as $CH_3CN$ show that similar overlaps exist. This raises the question of whether the masers are perhaps not directly associated with the thermal methanol in the hot core.

If the masers are directly associated with thermal methanol in hot cores, it means that the different velocity features seen in typical maser spectra are due to sampling in velocity space of the hot core methanol. Suppose now we have $N_t$ *identical* hot cores having associated masers with the $i$th core having $n_i$ maser features. If the masers sample the thermal methanol in the hot core in velocity space, it follows that the distribution of rest frame maser velocities will be a Gaussian with the same velocity dispersion as that of the thermal methanol line. In reality, however, hot cores have different physical properties and are therefore characterized by different velocity dispersions. In such a case the observed distribution of rest frame maser velocities is the result of a sampling from $N_t$ Gaussians such that $n_i$ velocities are sampled from the $i$th Gaussian which is characterized by a formal standard deviation $\sigma_i$. One way then to test the hypothesis that the masers sample the hot core gas would be to construct an average expected distribution by performing the above sampling with a Monte Carlo procedure and to compare it with the observed distribution. A simpler and perhaps more natural way, however, is to consider the dimensionless quantity defined by

$$V = (v_{\rm maser} - v_0)/\sigma \quad (1)$$

where $v_{\rm maser}$ is the LSR velocity of a maser feature and $v_0$ is the LSR systemic velocity of the core. $\sigma$ is the velocity dispersion of the thermal methanol as characterized by the formal standard deviation of a Gaussian line profile. If the masers are indeed sampling the thermal gas, it then follows, from standard statistics, that applying Eq. (1) to the $N_i$ maser features of the $i$th core which has a velocity dispersion characterized by $\sigma_i$, is to transform the observed maser velocities to that sampled from a standard $N(0, 1)$ velocity profile. Since this applies to every core in the sample it follows that the distribution of $V$ for all the maser features associated with all the cores in the sample should have a $N(0, 1)$ distribution. Should the masers not sample the thermal gas in velocity then the distribution of $V$ will not be an $N(0, 1)$ distribution. The quantity $V$ therefore acts as a test statistic which, under the null hypothesis that the masers sample the thermal velocities of the gas, has a $N(0, 1)$ distribution.

The relevant question now is as to what values of $\sigma$ will lead to a $N(0, 1)$ distribution for $V$ for the given set of 337 maser rest frame velocities? To answer this question we used the measured values of $\sigma$ for the CS(2−1) line and determined by trial and error by which factor these values must be multiplied such that the distribution of $V$ has a standard deviation of 1. It was found that multiplying the CS(2−1) $\sigma$'s with a factor of 3.5 results in $V$ having a standard deviation of 1. This implies, if the masers are sampling the thermal methanol in hot cores, that the mean velocity dispersion of the thermal methanol as measured by the standard deviation should be about 6.5 km s$^{-1}$. This translates to a *mean FWHM* of 15.6 km s$^{-1}$.

A search of the literature showed that such large values for the *FWHM* of typical hot core molecules do not occur. Due to the fact that a systematic survey of thermal methanol toward methanol maser sources does not exist and that thermal methanol data toward high mass star forming regions is also rather sparse, will we use methyl cyanide as a typical hot core molecule. However, in doing so we keep in mind that methanol is an oxygen bearing molecule while methyl cyanide is a nitrogen bearing molecule, and that this difference might also be reflected in the kinematics of the regions where the two types of molecules are formed. Using the data of Hatchell et al. (1998) we found an average *FWHM* of 8.0 km s$^{-1}$ for methyl cyanide and 6.3 km s$^{-1}$ for methanol. The standard deviations on the *FWHM* for these cases are 3.3 and 2.0 km s$^{-1}$ respectively, suggesting that the distributions of velocity dispersion for methyl cyanide and methanol are too narrow to explain the observed velocities of the methanol masers.

**Table 1.** Data of observed sources.

| Name | $V_{\rm lsr}$ | $\sigma$ | Maser velocities | | | | | | | | | | |
|---|---|---|---|---|---|---|---|---|---|---|---|---|---|
| | km s$^{-1}$ | km s$^{-1}$ | km s$^{-1}$ | | | | | | | | | | |
| G08.671-0.354 | 33.7 | 1.6 | 39.2 | | | | | | | | | | |
| G09.990-0.030 | 48.9 | 1.7 | 47.9 | 47.0 | 46.3 | 43.0 | 41.9 | 40.8 | | | | | |
| G10.313-0.152 | 14.7 | 1.0 | 11.4 | 12.2 | 13.0 | 14.3 | 15.5 | 16.7 | 20.0 | | | | |
| G10.626-0.383 | –3.4 | 2.8 | –8.9 | –8.0 | –7.2 | –6.0 | –0.3 | 0.8 | 2.1 | 3.9 | 4.8 | 5.8 | |
| G10.632-0.337 | –3.9 | 1.7 | –13.0 | –11.7 | –10.9 | –9.4 | –8.1 | –7.8 | –6.5 | –5.0 | –1.3 | –0.4 | |
| G10.962-0.016 | 21.0 | 2.1 | 24.7 | 24.4 | | | | | | | | | |
| G11.030+0.060 | 15.9 | 1.9 | 16.0 | 20.5 | | | | | | | | | |
| G11.500-1.500 | 10.6 | 1.3 | 16.2 | 15.3 | 14.8 | 14.3 | 13.4 | 13.0 | 10.0 | 8.9 | 8.0 | 7.2 | 6.7 | 6.3 |
| G11.900-0.140 | 37.8 | 2.7 | 40.0 | 42.6 | 43.1 | 43.7 | | | | | | | |
| G11.992-0.275 | 59.5 | 2.2 | 60.2 | | | | | | | | | | |
| G12.200-0.120 | 27.3 | 2.1 | 26.2 | 29.5 | 30.0 | 30.1 | 30.6 | 31.4 | | | | | |
| G12.209-0.103 | 24.2 | 2.7 | 19.5 | 20.4 | | | | | | | | | |
| G14.104+0.093 | 9.3 | 2.2 | 5.0 | 5.4 | 5.8 | 6.5 | 7.0 | 8.0 | 10.1 | 10.6 | 13.2 | 13.7 | 15.1 | 16.2 |
| G15.033-0.677 | 19.8 | 1.9 | 21.0 | 22.8 | 23.2 | | | | | | | | | |
| G16.582-0.047 | 59.3 | 1.4 | 68.6 | 63.9 | 61.9 | 59.3 | 58.4 | 57.0 | | | | | | |
| G16.868-2.158 | 17.5 | 2.0 | 14.7 | 16.9 | 18.4 | | | | | | | | | |
| G17.017-2.400 | 19.8 | 1.3 | 20.5 | 23.3 | | | | | | | | | | |
| G17.640+0.160 | 22.5 | 1.3 | 19.7 | | | | | | | | | | | |
| G18.836-0.304 | 42.5 | 1.8 | 41.1 | 43.5 | 42.5 | | | | | | | | | |
| G19.470+0.017 | 18.8 | 3.1 | 20.6 | 21.3 | 22.3 | 24.1 | | | | | | | | |
| G19.488+0.140 | 24.4 | 1.7 | 24.2 | 23.0 | 22.4 | 21.5 | 20.9 | 18.0 | | | | | | |
| G19.610-0.132 | 57.6 | 1.8 | 56.2 | 52.4 | 50.2 | | | | | | | | | |
| G20.230+0.070 | 71.0 | 2.4 | 60.6 | 61.3 | 68.6 | 70.9 | 71.6 | 73.1 | 74.2 | 75.5 | 76.0 | 77.3 | | |
| G22.358+0.064 | 84.6 | 1.6 | 85.0 | 80.0 | 77.0 | | | | | | | | | |
| G22.430-0.160 | 28.7 | 1.8 | 23.4 | 24.6 | 25.0 | 25.5 | 29.5 | 32.6 | 33.2 | 35.0 | 38.2 | 39.6 | | |
| G23.245-0.240 | 63.2 | 2.1 | 63.9 | 64.7 | 66.0 | | | | | | | | | |
| G23.457+0.068 | 84.0 | 1.3 | 88.0 | 87.0 | 84.8 | 82.0 | | | | | | | | |
| G24.330+0.140 | 112.8 | 2.3 | 108.2 | 110.1 | 111.9 | 113.0 | 114.3 | 115.3 | | | | | | |
| G24.489-0.046 | 110.1 | 2.1 | 109.2 | 111.3 | 114.5 | 115.3 | | | | | | | | |
| G24.790+0.080 | 110.7 | 2.0 | 107.5 | 107.8 | 109.3 | 110.1 | 111.6 | 112.0 | 113.0 | 113.8 | 114.5 | | | |
| G24.845+0.091 | 109.2 | 1.8 | 114.6 | 113.9 | 113.3 | 112.2 | 111.7 | 110.8 | 110.3 | 109.7 | 107.9 | 107.6 | 106.7 | |
| G25.720+0.050 | 100.5 | 2.1 | 89.7 | 91.1 | 91.8 | 92.3 | 93.5 | 94.5 | 94.8 | 95.4 | 96.3 | 99.9 | | |
| G26.610-0.220 | 107.8 | 1.1 | 103.7 | 108.2 | 111.9 | 112.3 | 113.2 | | | | | | | |
| G27.280+0.150 | 31.8 | 2.4 | 35.0 | | | | | | | | | | | |
| G27.360-0.160 | 92.2 | 1.8 | 88.5 | 91.7 | 97.4 | 98.4 | 98.9 | 99.7 | 100.2 | 101.5 | 104.0 | | | |
| G28.840-0.232 | 96.0 | 1.5 | 99.8 | 91.7 | 90.9 | | | | | | | | | |
| G29.860-0.050 | 100.4 | 1.5 | 99.1 | 100.6 | 101.0 | 101.5 | 101.9 | 103.0 | 103.6 | | | | | |
| G29.956-0.017 | 97.3 | 1.7 | 104.5 | 103.9 | 103.4 | 102.5 | 101.8 | 101.2 | 100.1 | 98.9 | 98.2 | 97.7 | 96.5 | 95.7 |
| G30.200-0.170 | 103.3 | 1.2 | 101.3 | 103.2 | 104.9 | 105.8 | 108.2 | 109.0 | 110.0 | 110.5 | | | | |
| G30.220-0.180 | 104.5 | 1.4 | 111.4 | 113.2 | 113.5 | | | | | | | | | |
| G30.536+0.018 | 48.0 | 1.8 | 43.2 | | | | | | | | | | | |
| G30.590-0.040 | 42.3 | 2.1 | 42.5 | 45.3 | | | | | | | | | | |
| G30.762-0.053 | 91.0 | 2.3 | 108.2 | 101.2 | 92.8 | 91.8 | 90.9 | 89.9 | 88.6 | 88.0 | 87.3 | 85.9 | | |
| G30.780+0.230 | 41.6 | 1.4 | 47.5 | 49.3 | | | | | | | | | | |
| G30.790-0.060 | 91.2 | 2.1 | 86.0 | 88.2 | 89.8 | 91.2 | 91.8 | | | | | | | |
| G32.089+0.091 | 95.2 | 1.4 | 92.8 | 94.5 | 95.4 | 98.3 | 99.5 | 100.8 | 101.0 | | | | | |
| G32.740-0.080 | 36.8 | 2.9 | 24.9 | 26.5 | 30.1 | 32.4 | 33.5 | 35.4 | 36.0 | 38.2 | 38.9 | 44.8 | | |
| G32.750-0.070 | 37.0 | 2.4 | 30.1 | 31.8 | 32.3 | 33.0 | 33.5 | 37.4 | 38.2 | 38.9 | 37.0 | 35.8 | 36.2 | |
| G33.090-0.070 | 100.5 | 1.1 | 95.5 | 97.5 | 100.0 | 102.1 | 104.0 | 105.1 | | | | | | |
| G33.417-0.004 | 74.8 | 1.6 | 102.1 | 102.4 | 104.8 | 105.1 | 106.1 | | | | | | | |
| G35.030+0.350 | 52.8 | 1.8 | 44.2 | 45.4 | 45.7 | | | | | | | | | |
| G36.110+0.550 | 75.9 | 1.4 | 70.4 | 72.0 | 73.0 | 74.4 | 76.1 | 82.2 | 84.0 | | | | | |
| G37.430+1.520 | 43.9 | 1.4 | 41.1 | | | | | | | | | | | |
| G43.790-0.120 | 44.0 | 2.8 | 39.4 | 39.9 | 40.3 | 43.0 | | | | | | | | |
| G45.070+0.130 | 59.1 | 2.1 | 57.8 | | | | | | | | | | | |
| G45.490+0.130 | 60.6 | 1.9 | 59.7 | | | | | | | | | | | |
| G49.488-0.380 | 59.5 | 3.8 | 52.2 | 56.2 | 58.1 | 59.3 | 59.9 | 60.7 | | | | | | |
| G49.570-0.270 | 52.6 | 2.0 | 58.0 | 59.3 | 62.8 | 63.8 | 64.9 | 66.0 | | | | | | |
| G59.780+0.060 | 22.5 | 1.0 | 14.4 | 16.0 | 17.2 | 19.7 | 20.5 | 21.9 | 24.9 | 27.3 | | | | |
| G73.060+1.080 | 0.7 | 0.8 | –2.9 | –2.5 | 6.0 | | | | | | | | | |
| G75.770+0.340 | –1.4 | 2.2 | –10.0 | –9.7 | –2.9 | –0.7 | –0.1 | 0.4 | | | | | | |
| G109.90+2.120 | –10.8 | 2.0 | –4.9 | –4.2 | –3.9 | –2.6 | –2.0 | | | | | | | |
| G111.50+0.780 | –57.4 | 1.8 | –61.5 | –60.9 | –59.2 | –58.1 | –57.5 | –56.4 | –52.9 | –48.9 | –48.5 | | | |

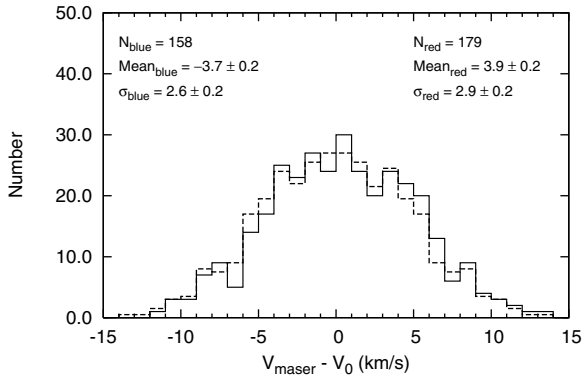


**Fig. 2.** Distribution of the rest frame radial velocities for 337 maser features in 63 maser sources (solid line). The statistical properties for the red- and blue shifted maser features are given in the figure and suggest that there is no difference between the red and blue shifted sides. The dashed line gives the average distribution. The means and standard deviations are in km s$^{-1}$.

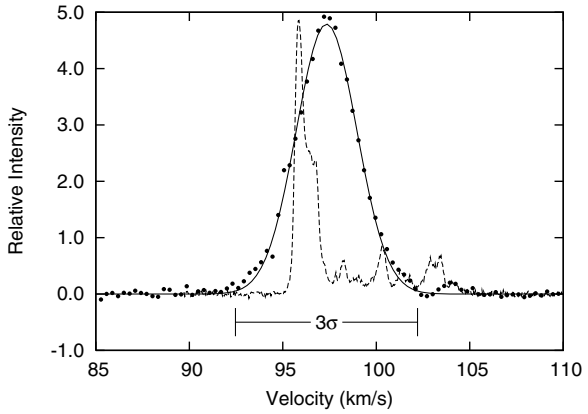


**Fig. 3.** Comparison of the CS(2−1) thermal line profile (filled circles = data, solid line = Gaussian fit) and the 6.7 GHz maser spectrum (dashed line) for G29.96-0.02.

Pankonin et al. (2001) detected $CH_3CN(12-11)$ from 25 candidate massive star forming regions. The average *FWHM* for their detections is 7.85 km s$^{-1}$ with a standard deviation of 3.0 km s$^{-1}$. Recently Purcell et al. (2006) survey a large number of southern methanol maser sources in $CH_3CN(6-5)$. For these measurements a mean *FWHM* of 5.0 km s$^{-1}$ with a standard deviation of 1.7 km s$^{-1}$ is found. Kalenskii et al. (2000) surveyed 30 high mass star forming regions in $CH_3CN(5-4)$ and $CH_3CN(6-5)$. The average *FWHM* for these two transitions is 5.6 km s$^{-1}$ and the standard deviation 3.4 km s$^{-1}$. Using the Bonn 100 m telescope Olmi et al. (1993) surveyed a number of hot cores in $CH_3CN(6-5)$, $CH_3CN(8-7)$, and $CH_3CN(12-11)$. The mean *FWHM*'s were respectively, 5.94, 6.23, and 6.16 km s$^{-1}$. Recent interferometric observations by Beltrán et al. (2005) gives a range of the *FWHM* for methyl cyanide from 6.1 to 9.77 km s$^{-1}$ for G31.41+0.31 and from 4.58 to 7.25 km s$^{-1}$ for G24.78+0.08. These values coincide with the range of values found from the abovementioned single dish observations. Thermal methanol emission in DR21 shows a *FWHM* ranging from 1.1 to 3.5 km s$^{-1}$ only (Liechti & Walmsley 1997) while in W3(OH/$H_2O$) the *FWHM* for methanol ranges from 2.2 to 4.6 km s$^{-1}$ (Sutton et al. 2004).

Considering the number of massive star forming regions involved in the abovementioned surveys and the agreement of the mean *FWHM*s for the different surveys, it is clear that the velocity dispersions associated with hot cores are not large enough to explain the rest frame velocities of the masers. The significant difference between the velocity dispersions observed and that required to explain the masers in terms of sampling the hot core methanol, suggest that the observed maser rest frame velocities most likely have a non-thermal origin.

To end this section we point out that Slysh et al. (1999b) considered the rest frame velocity distribution of the strongest masers features for 157 maser sources. Qualitatively these authors found a similar result to that presented above viz. that the dispersion of rest frame maser velocities is significantly larger than the thermal velocity dispersion, even of hot cores.

### 3.2. External generated planar shocks

That methanol masers might be associated with shocks was proposed by a number of authors e.g. Sobolev & Deguchi (1994), Hartquist et al. (1995) and Walsh et al. (1998). More recently the planar shock model was further developed by Dodson et al. (2004) to explain the velocity gradients they observed in the clusters of maser spots with linear morphologies. Basically the hypothesis is that class II methanol masers arise behind an externally generated planar shock propagating into a rotating star forming core (see Fig. 15 of Dodson et al. 2004). In this model the rotation of the core is required to explain the observed velocity gradients. We note the following consequence of this model that is relevant to our present discussion.

An important aspect that any model of the masers must be able to explain is the velocity range covered by methanol masers. Malyshev & Sobolev (2003) and Slysh et al. (1999b) showed that in a significant fraction of the maser sources the velocity range is greater than 5 km s$^{-1}$. This is also valid for the maser clusters with a linear morphology (Walsh et al. 1998; Phillips et al. 1998). The question now is whether the planar shock model of Dodson et al. (2004) can explain the observed velocity ranges of methanol masers. An examination of this model will show that the maximum difference in velocity between two maser features is obtained when *simultaneously* the following conditions apply: (i) the rotation axis of the core is in the plane of the sky; (ii) the plane of the shock is perpendicular to the rotation axis; (iii) the shock crosses the middle of the core; and (iv) when the maser features are located at the edge of the core. Applying these conditions to a maser emitting region, the linear dimensions of which typically is 0.03 pc (Caswell 1997; Phillips et al. 1998), it follows, assuming solid body rotation, that a velocity gradient greater than 150 km s$^{-1}$ pc$^{-1}$ is required to exist in the masing region to explain a velocity range of only 5 km s$^{-1}$ in the maser features. The question now is whether a velocity gradient in excess of 150 km s$^{-1}$ pc$^{-1}$ is in agreement with the observed rotation of molecular cloud cores.

Observationally rotation of cloud cores will be manifested as velocity gradients. However, not all observed velocity gradients should be interpreted as being due to rotation since e.g. aspherical outflows may also give rise to velocity gradients. Keeping this in mind we note the following: Pirogov et al. (2003) mapped massive molecular cloud cores in $N_2H^+(1-0)$ and found velocity gradients in the range 0.09−2.9 km s$^{-1}$ pc$^{-1}$ with a mean of 0.5 km s$^{-1}$ pc$^{-1}$ while Goodman et al. (1993) found velocity gradients ranging between 0.2 and 4.0 km s$^{-1}$ for lower mass molecular cores. Phillips (1999) compiled a data base of cloud rotation measures which include also rotation rates for clumps in molecular clouds. For the latter the rotation rates range from $0.65 \times 10^{-14}$ s$^{-1}$ to $125 \times 10^{-14}$ s$^{-1}$. Of the 26 clumps, 24 have rotation rates less than $10^{-13}$ s$^{-1}$ with a mean of $3.1 \times 10^{-14}$ s$^{-1}$ which corresponds to a velocity gradient

of ∼1.0 km s$^{-1}$ pc$^{-1}$. It is interesting to note that the clump with the largest rotation rate has a linear dimension of 0.04 pc, similar to that of methanol maser emitting regions. The corresponding velocity gradient for this clump is ∼39 km s$^{-1}$ pc$^{-1}$, which still is significantly smaller than what is required to explain a velocity range of 5 km s$^{-1}$.

Using the typical linear dimension of a masing region and the maximum observed velocity gradient of 39 km s$^{-1}$ pc$^{-1}$, the maximum velocity range predicted by this model is only 1.14 km s$^{-1}$. Thus, even if only a fraction of the observed velocity gradients in the abovementioned references is due to rotation, it would seem as if typical rotation rates are too small to explain the observed velocity ranges of methanol masers. It follows therefore that, within the framework of the planar shock model, to explain the typical maser spectrum with numerous features covering a velocity range which, in some cases may be up to 20 km s$^{-1}$, would require multiple shocks with different velocities, inclination angles and incident from different directions, to propagate through the core. In particular, to produce the observed distribution of rest frame maser velocities as well as the linear arrangements of maser spots with a well defined velocity gradient would require multiple shocks to propagate through the core with exactly the right velocities, directions, and positions relative to each other. Such a coincidence seems to be a highly unlikely situation.

Clearly then, to explain the observed velocity ranges of methanol masers requires some distinct spatio-kinematic structures other than external generated planar shocks propagating through a core.

### 3.3. Disks

The hypothesis that the masers originate in disks was originally proposed by Norris et al. (1993) and later again by Norris et al. (1998). Their model is a simple kinematic model in which the individual masers are located at more or less the same distance from the disk center. The projection of the orbital velocity in the disk on the line-of-sight gives rise to red- and blue shifted emission features. This is the most simple model to explain the observed velocity gradients associated with the linear spatial distribution of maser spots seen in high resolution maps of some methanol maser sources.

We first investigate whether the simple disk model can give rise to a distribution of rest frame velocities which is similar to that observed (Fig. 2). The geometry of this scenario is simple enough to investigate this possibility. For this purpose we constructed a Monte Carlo model in which individual masers are uniformly distributed in an annulus within a Keplerian-like disk around a star of mass $M$. The masses of the stars were selected at random from a Salpeter IMF between 10 and 50 $M_\odot$. The disk mass was taken as 0.35 of the stellar mass, which is about the average of the ratio of the estimated disk to stellar mass for the currently known candidate disks associated with young high mass stars (Cesaroni et al. 2006). The minimum distance from the star at which the masers can occur should be such that it can give rise to the maximum observed rest frame velocity of the masers when the disk is viewed edge-on. For the star + disk system this distance was calculated from $R_{\rm min} = (3\pi/4)GM_{\rm t}/v^2_{\rm max}$ (Mestel 1963; Cesaroni et al. 2006) where $M_{\rm t}$ is the total mass. From Fig. 2 we note that the maximum rest frame velocity of the maser features is about 15 km s$^{-1}$. For a 10 $M_\odot$ star we then have $R_{\rm min} \simeq 80$ AU. The outer radius, $R_{\rm max}$, of the annulus in which the masers can occur has been left as the only free parameter. We also assumed that the inclination angle of the disk relative to the line-of-sight has a uniform distribution between 0° (edge-on) and 90° (face-on).

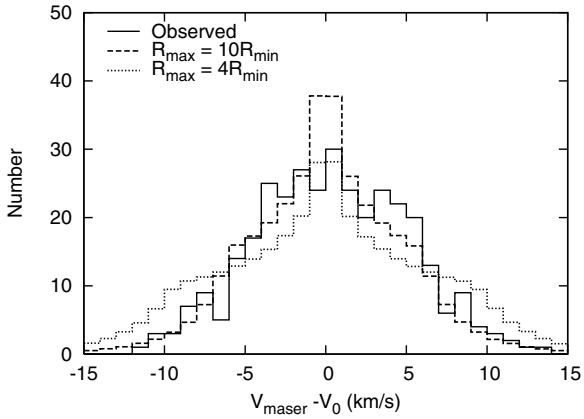


**Fig. 4.** Comparison between the observed and the Keplerian disk model rest frame velocity distributions. For the model we present two cases, viz. where the outer radius of the annulus was respectively four and 10 times the inner radius where the inner radius is the radius at which the orbital velocity in the disk is 15 km s$^{-1}$. See text for more details on the model.

The resulting distribution of rest frame maser velocities for $R_{\rm max} = 4R_{\rm min}$ and $R_{\rm max} = 10R_{\rm min}$ are compared in Fig. 4 with the observed distribution. It is remarkable that for $R_{\rm max} = 10R_{\rm min}$ this simple single parameter model can produce a distribution of rest frame velocities that is very similar to the observed distribution. The case for $R_{\rm max} = 4R_{\rm min}$ is also shown as an example to illustrate the effect of varying $R_{\rm max}$. Narrowing the annulus while keeping $R_{\rm min}$ such that the orbital velocity at that radius is 15 km s$^{-1}$, obviously has to have the effect of overemphasizing the higher velocities relative to lower velocities. On the other hand (not shown), making the annulus too large has the effect of including a too large surface area of the disk where the orbital velocities are less than only a few kilometers per second. In this case the peak (low velocities) of the distribution is overemphasized relative to the higher velocity tails.

A notable difference between the model and observed distributions is that in the model the peak of the distribution is more localized and higher than what is observed for real maser sources. However, we have to note that this simple model does not consider radiative transfer effects and variations of maser brightness due to variation in path lengths. Norris et al. (1998) argue that ultra compact HII regions are still optically thick at 6.7 GHz and that maser emission propagating perpendicular to the disk may be attenuated severely in propagating through the HII region. In this idealized model we also have infinitely good velocity resolution and did not take into account the fact that the maser lines will converge and blend in velocity space as the inclination angle of the disk approaches 90°. We therefore may have counted to many maser lines in this case. It is uncertain to what extent this might be a real effect.

The fact that this simple kinematic model is able to easily reproduce the observed kinematic properties of the masers should not be overinterpreted and taken as final proof that the masers originate in disks. Real disks are certainly much more complex and might lead to deviations from the predictions of this simple model. It also still needs to be shown theoretically and observationally that the physical and chemical conditions in certain parts of the disks are favourable for the existence of the masers. The assumption that the masers are uniformly distributed in an annulus certainly is also not completely realistic. However, in spite

of this criticism, from the perspective of the kinematic properties of the masers the fact that the observed distribution of rest frame maser velocity can be repoduced with a simple Keplerian-like disk model cannot simply be ignored. It certainly is in strong support of the disk hypothesis of Norris et al. (1993) and Norris et al. (1998) and in this sense can explain some of the observed kinematic properties of the masers.

The next question to be answered is whether there are examples of disks or disklike structures associated with high mass stars for which the rotational velocity is such that the quantity $V$ defined above, can have values of a couple of times the velocity dispersion of the thermal gas. Searching the literature we found two such systems. The first is AFGL 5142. Zhang et al. (2002) identified a 1800 AU compact structure in $NH_3$ with a total velocity width at the $3\sigma$ level of about 15 km s$^{-1}$ and the kinematics of which is consistent with rotation. This structure is embedded in a cold extended core with a *FWHM* of 2.3 km s$^{-1}$. Using the total velocity width it is found that the maximum rotation velocity is 7.7 times that of the velocity dispersion of the cold extended core. The second case is that of IRAS 20126+4104. This source has been studied by Cesaroni et al. (1997). These authors found a molecular clump centered on the $H_2O$ masers associated with the IRAS source. The center of the clump also seems to be the origin of a molecular bipolar outflow to be clearly seen in the interferometric maps in $HCO^+(1-0)$. A flattened structure elongated in the direction perpendicular to the outflow axis is seen in the $CH_3CN(5-4)$ line which the authors interpret as a rotating disk with a very young star at its center. Using the average $V_{\rm lsr}$ and *FWHM* of the $HCO^+$, HCN, CS, $C^{34}S$, and $^{13}CO$ lines toward the center position of the Pico Veleta 30-m maps and their Fig. 10, we found that in the cloud rest frame the maximum line-of-sight velocity for the rotating flattened structure is about 3.5 times the velocity dispersion of the surrounding gas. Following a similar analysis on the data of Beltrán et al. (2005), we found that in the cloud rest frame the maximum line-of-sight velocities for the rotating toroids in G31.41+0.31 and G24.78+0.08 are respectively 1.5 and 1.2 times the velocity dispersion of the surrounding gas.

These results show that there are rotating structures associated with young high mass stars that produce rest frame line-of-sight velocities which are a couple of times the velocity dispersion of the surrounding gas. An unanswered question at this point is whether in general disks can explain the large velocity ranges of up to 20 km s$^{-1}$ for the methanol masers as seen in many sources. This would imply that most disks are seen edge-on which is a most unlikely situation. Goodman et al. (1993) found no definite trend in the spatial orientation of the rotation axes of the cores which might also apply to disks inside cores.

### 3.4. Outflows

It is well established that the probability to detect an outflow toward a methanol maser source is high (see e.g. Codella et al. 2004). Of the four possible scenarios for the origin of the methanol masers, outflows are certainly the most complex with too many unknown parameters so as to construct a simple model as in the case of disks. The complexity is mainly due to the widely different geometric configurations of outflows associated with high mass star formation. See e.g. Shepherd (2005) for a general discussion and Sutton et al. (2001), Bartkiewicz et al. (2005), and De Buizer (2006) for specific examples of methanol maser sites.

In terms of our sample of sources we note the following: of the 63 sources, 20 have clear indications of high velocity wings in the CS(2−1) spectra, generally being interpreted as due to outflows. Counting blue- and redshifted wings separately there are 32 wings equally divided between the two groups. Using the CS(2−1) data we estimated the maximum line-of-sight velocity with respect to the systemic velocity for each of the wings and divided it by the velocity dispersion of the CS(2−1) line as obtained from the Gaussian fitting as described earlier. In terms of the quantity $V$ defined above, we found that the average rest frame maximum velocity for both the red- and blue-shifted is $5.2\sigma$. For the red-shifted wings, the minimum and maximum offsets are $3.4\sigma$ and $7.5\sigma$ respectively while for the blue-shifted wings the corresponding values are $3.3\sigma$ and $7.6\sigma$. These numbers clearly show that outflows have high enough velocities to account for the observed offset of maser velocities from the systemic velocities and, at face value, therefore cannot be ignored as a possible environment where the masers originate.

If the methanol masers are indeed associated with outflows, then, at least, on the basis of the pumping conditions it can be said that the 6.7 GHz methanol masers are not physically associated with water masers which are generally considered to be associated with outflows. Menten (1996) discusses the conditions required to excite OH, water and methanol masers and show that although the three species can coexist in the gas phase, OH and methanol maser emission cannot arise from the same region as that of water masers. From a kinematic point of view it is also well known (see e.g. Sridharan et al. 2002) that the velocity range covered by water maser features is larger than that of methanol masers. Using the water maser data of Hofner & Churchwell (1996) for the sources G5.89-0.38, G8.67-0.36, G9.62+0.19, G10.47+0.03, G10.62-0.38, G11.94-0.62, G12.21-0.10, G29.96-0.02, G31.41+0.31, G34.26+0.15, G37.55-0.11, G43.18-0.52, G43.89-0.78, G45.07+0.13 and G75.78-0.34 (for these sources we could find reliable systemic velocities in the literature) we found for the 82 water maser features belonging to the above sources, that the standard deviation of the rest frame maser velocities is 13.7 km s$^{-1}$. This has to be compared with the standard deviation of 4.8 km s$^{-1}$ for the 337 methanol maser features we have used. The distribution of rest frame maser velocities for water masers is therefore significantly broader than for the methanol masers and reflects the differences in the kinematics of the regions where the two types of masers originate. This difference in kinematics of water masers on the one hand and OH and methanol masers on the other hand, is also considered by Menten (1996) as pointing to the fact that they originate in different regions.

Thus, if the methanol masers are associated with outflows, it must be in a completely different physical region than where the water masers operate and the kinematics be such that, amongst other things, it gives rise the observed distribution of rest frame maser line-of-sight velocities (Fig. 2).

## 4. Discussion and conclusions

At least two points of criticism can be raised against our ensemble approach to determine where in the circumstellar environment the masers arise. The first is that all the information contained in the spatial distribution of maser features is lost. It certainly is possible that the physical and chemical conditions required for the masers to operate (see Cragg et al. 2005) indeed exist in certain parts of hot cores, in post-shock gas, in outflows, and in disks and that both the spatial and kinematic information are required to determine where in the circumstellar environment the masers arise. However, Beuther et al. (2002) concluded that even with having such information available, it is very difficult

to come to a definite conclusion about where in the circumstellar environment the masers arise. Having spatial and kinematic information available, however, does not seem to guarantee an answer to the problem.

The second point of criticism that can be raised against the above procedure is the assumption of the masers being associated with only one of the four possible environments. This assumption may not be correct. As noted above, it certainly is possible that in an individual source the correct physical and chemical conditions to excite the masers might exist at various places in the circumstellar environment and that, in principle, the masers are not associated with only one of the four possibilities discussed above. If this is indeed in general the case it might explain the difficulty in determining where the masers arise since modelling of the kinematics of maser spots in individual sources usually assumes all the maser spots to be associated with the same physical structure, e.g. on the surface of a conical bipolar outflow (see e.g. Moscadelli et al. 2002). If in fact some of the masers don't arise in disks or in clumps following Keplerian orbits around the exciting star but elsewhere in the circumstellar environment, it means that the distribution of rest frame maser velocities is some weighted mixture of a number of distributions. It is not possible with the above ensemble approach to determine in any way whether this is the case and if so, what fraction of the masers are associated with each component. However, it would be a remarkable coincidence that an arbitrary weighted mixture of a number of distributions gives rise to a distribution of rest frame velocities that can be fitted so well with that of a Keplerian-like disk.

In view of our evaluation of the four scenarios in terms of the kinematics of the masers for where in the circumstellar environment the masers arise, do we conclude as follows:

- If the masers were to sample thermal methanol in hot cores, it would have required the observed *FWHM* of methanol lines to be significantly larger than what is observed for any of the typical hot core molecules. Since this is not the case this very stongly suggests that the masers are most likely not associated with thermal methanol in hot cores.
- The model in which the masers arise in the post-shock gas behind an external generated planar shock propagating into a rotating core cannot explain one of the most basic observed kinematic properties of the masers, i.e. the velocity range covered by the masers. It is thus doubtfull that this model is the correct model with which to explain the 6.7 GHz methanol masers.
- The results of a simple Keplerian-like disk model in which the masers are located in an annulus rather than a thin ring as was originally proposed by Norris et al. (1993) and Norris et al. (1998) is consistent with the observed rest frame distribution of maser velocities. For a given stellar mass and a disk-to-star mass ration of 0.35, the inner radius of the annulus is determined by the maximum observed rest frame maser velocity. This is about 80 AU for a 10 $M_{\odot}$ star. It still needs to be shown that the conditions necessary to pump the masers do exist in disks.
- Due to the diversity of outflows it is not possible to construct a representative model to compare with the observations and thereby to determine whether the distribution of rest frame velocities as shown in Fig. 2 is uniquely due to Keplerian-like disks or whether it can also be due to outflows.

*Acknowledgements.* We thank an anonymous referee for constructive comments.
D.J.v.d.W. was supported by the National Research Foundation under Grant number 2053475.

## References

Bartkiewicz, A., Szymczak, M., & van Langevelde, H. J. 2005, A&A, 442, L61
Beltrán, M. T., Cesaroni, R., Neri, R., et al. 2005, A&A, 435, 901
Beuther, H., Walsh, A., Schilke, P., et al. 2002, A&A, 390, 289
Bronfman, L., Nyman, L.-A., & May, J. 1996, A&AS, 115, 81
Caswell, J. L. 1997, MNRAS, 289, 203
Caswell, J. L., Vaile, R. A., Ellingsen, S. P., Whiteoak, J. B., & Norris, R. P. 1995, MNRAS, 272, 96
Cesaroni, R., Felli, M., Testi, L., Walmsley, C. M., & Olmi, L. 1997, A&A, 325, 725
Cesaroni, R., Galli, D., Lodato, G., Walmsley, C. M., & Zhang, Q. 2006, [arXiv:astro-ph/0603093]
Codella, C., Lorenzani, A., Gallego, A. T., Cesaroni, R., & Moscadelli, L. 2004, A&A, 417, 615
Cragg, D. M., Sobolev, A. M., & Godfrey, P. D. 2002, MNRAS, 331, 521
Cragg, D. M., Sobolev, A. M., & Godfrey, P. D. 2005, MNRAS, 360, 533
De Buizer, J. M. 2003, MNRAS, 341, 277
De Buizer, J. M. 2006, ApJ, 642, L57
De Buizer, J. M., Radomski, J. T., Telesco, C. M., & Pina, R. K. 2005, in IAU Symp., 227 (Cambridge University Press), 180
Dodson, R., Ojha, R., & Ellingsen, S. P. 2004, MNRAS, 351, 779
Durisen, R. H., Mejia, A. C., Pickett, B. K., & Hartquist, T. W. 2001, ApJ, 563, L157
Ellingsen, S. P. 2006, ApJ, 638, 241
Goodman, A. A., Benson, P. J., Fuller, G. A., & Myers, P. C. 1993, ApJ, 406, 528
Hartquist, T. W., Menten, K. M., Lepp, S., & Dalgarno, A. 1995, MNRAS, 272, 184
Hatchell, J., Thompson, M. A., Millar, T. J., & MacDonald, G. H. 1998, A&AS, 133, 29
Hofner, P., & Churchwell, E. 1996, A&AS, 120, 283
Kalenskii, S. V., Promislov, V. G., Alakoz, A., Winnberg, A. V., & Johansson, L. E. B. 2000, A&A, 354, 1036
Liechti, S., & Walmsley, C. M. 1997, A&A, 321, 625
Malyshev, A. V., & Sobolev, A. M. 2003, Astronomical and Astrophysical Transactions, 22, 1
Menten, K. 1991, in Atoms, Ions and Molecules: New Results in Spectral Line Astrophysics, ed. A. D. Haschick, & P. T. P. Ho, ASP Conf. Ser., 16, 119
Menten, K. M. 1996, in Molecules in Astrophysics: Probes & Processes, ed. E. F. van Dishoeck, IAU Symp., 178, 163
Mestel, L. 1963, MNRAS, 126, 553
Minier, V., Booth, R. S., & Conway, J. E. 2000, A&A, 362, 1093
Minier, V., Conway, J. E., & Booth, R. S. 2001, A&A, 369, 278
Moscadelli, L., Menten, K. M., Walmsley, C. M., & Reid, M. J. 2002, ApJ, 564, 813
Norris, R. P., Whiteoak, J. B., Caswell, J. L., Wieringa, M. H., & Gough, R. G. 1993, ApJ, 412, 222
Norris, R. P., Byleveld, S. E., Diamond, P. J., et al. 1998, ApJ, 508, 275
Olmi, L., Cesaroni, R., & Walmsley, C. M. 1993, A&A, 276, 489
Pankonin, V., Churchwell, E., Watson, C., & Bieging, J. H. 2001, ApJ, 558, 194
Pestalozzi, M. R., Minier, V., & Booth, R. S. 2005, A&A, 432, 737
Phillips, C. J., Norris, R. P., Ellingsen, S. P., & McCulloch, P. M. 1998, MNRAS, 300, 1131
Phillips, J. P. 1999, A&AS, 134, 241
Pirogov, L., Zinchenko, I., Caselli, P., Johansson, L. E. B., & Myers, P. C. 2003, A&A, 405, 639
Purcell, C. R., Balasubramanyam, R., Burton, M. G., et al. 2006, MNRAS, 198
Shepherd, D. 2005, in IAU Symposium, ed. R. Cesaroni, M. Felli, E. Churchwell, & M. Walmsley, 237
Slysh, V. I., Val'Tts, I. E., Kalenskii, S. V., & Larionov, G. M. 1999a, Astron. Rep., 43, 657
Slysh, V. I., Val'tts, I. E., Kalenskii, S. V., et al. 1999b, A&AS, 134, 115
Sobolev, A. M., & Deguchi, S. 1994, A&A, 291, 569
Sobolev, A. M., Wallin, B. K., & Watson, W. D. 1998, ApJ, 498, 763
Sridharan, T. K., Beuther, H., Schilke, P., Menten, K. M., & Wyrowski, F. 2002, ApJ, 566, 931
Sutton, E. C., Sobolev, A. M., Ellingsen, S. P., et al. 2001, ApJ, 554, 173
Sutton, E. C., Sobolev, A. M., Salii, S. V., et al. 2004, ApJ, 609, 231
Szymczak, M., Hrynek, G., & Kus, A. J. 2000, A&AS, 143, 269
van der Walt, J. 2005, MNRAS, 360, 153
Wallin, B. K., Watson, W. D., & Wyld, H. W. 1998, ApJ, 495, 774
Walsh, A. J., Burton, M. G., Hyland, A. R., & Robinson, G. 1998, MNRAS, 301, 640
Xu, Y., Zheng, X.-W., & Jiang, D.-R. 2003, Chin. J. A&A, 3, 49
Zhang, Q., Hunter, T. R., Sridharan, T. K., & Ho, P. T. P. 2002, ApJ, 566, 982